JOURNAL OF THEORETICAL AND APPLIED MECHANICS
56, 3, pp. 829-839, Warsaw 2018
DOI: 10.15632/jtam-pl.56.3.829

MODELLING OF FGM PLATES

Grzegorz Jemielita
Warsaw University of Life Sciences, Faculty of Civil and Environmental Engineering, Warsaw, Poland
e-mail: g.jemielita@il.pw.edu.pl

Zofia Kozyra
Warsaw University of Technology, Faculty of Civil Engineering, Warsaw, Poland
e-mail: z.kozyra@il.pw.edu.pl

The paper presents formulation of the problem of layered plates composed of two various isotropic materials. We assume that the first material M_1 is characterized by the following parameters: Young's modulus E_1 and Poisson's ratio ν_1, whereas the second one by E_2 and ν_2, respectively. Let us consider two modelling cases for functionally graded material (FGM) plates. These cases are related to an appropriate distribution of the material within two-layer and three-layer systems. Our objective is to compare the stiffness of both the two-layer and there-layer plates with the FGM plate containing various proportions between the material components M_1 and M_2.

Keywords: modelling, layer plate, FGM plate, stiffness of the plate

1. Introduction

The effect of a continuous change in the plate properties (through the thickness) can be obtained in various ways. The overall properties of FMGs are unique and differ from any of the individual material forming it (Mahamood *et al.*, 2012).

Usually, we assume isotropic plates with variation of two constituents: ceramic and metal (Mokhtar *et al.*, 2009). Another possibility is to assume aluminium-alumina FGM plates (Rohit Saha and Maiti, 2012).

Thus, the created plate material is inhomogeneous with both the composition and material properties varying smoothly through thickness of the plate. The material properties along the thickness direction of the FGM plate vary in accordance to a power-law function, exponential function, sigmoid function, etc. Another modelling examples known in the literature are related to asymptotic and tolerance modelling (Woźniak, 1995; Nagórko, 1998, 2010; Wągrowska and Woźniak, 2015; Woźniak *et al.*, 2016).

Most material properties through the plate thickness are expressed by

$$p(z) = (p_1 - p_2)f(z) + p_2 \tag{1.1}$$

where

$$f(z) = \Big(\frac{1}{2} + \frac{z}{h}\Big)^n \qquad\qquad p = \rho, E, \nu \tag{1.2}$$

where h is the plate thickness, the subscripts 1 and 2 indicate the top $z = h/2$ and bottom $z = -h/2$ surfaces, E – Young's modulus, ν – Poisson's ratio, ρ is mass density, n – material parameter (Reddy, 2000; Efraim, 2011; Kim and Reddy, 2013; Kumar *et al.*, 2011). Mokhtar *et al.* (2009) use the following definition of the function $p(z)$

$$p(z) = \begin{cases} f_1(z)p_c + [1 + f_1(z)]p_m & \text{for} \quad 0 \leqslant z \leqslant \dfrac{h}{2} \\ f_2(z)p_c + [1 + f_2(z)]p_m & \text{for} \quad -\dfrac{h}{2} \leqslant z \leqslant 0 \end{cases} \tag{1.3}$$

where

$$f_1(z) = 1 - \frac{1}{2}\Big(1 - \frac{2z}{h}\Big)^n \qquad f_2(z) = \frac{1}{2}\Big(1 + \frac{2z}{h}\Big)^n \tag{1.4}$$

Delale and Erdogan (1983) and Rohit Saha and Maiti (2012) used an exponential function in order to describe the variation of Young's modulus in the following form

$$E(z) = E_m \exp\Big(z + \frac{h}{2}\Big) \qquad B = \frac{1}{h} \ln \frac{E_c}{E_m} \qquad -\frac{h}{2} \leqslant z \leqslant \frac{h}{2} \tag{1.5}$$

In this work, we present a new FGM plate model formulated by using an appropriate modelling related to double-layer and three-layer plates.

2. Modelling of an FGM plate developed from a two-layer plate

Let us assume a two-layer plate whose scheme is shown in Fig. 1.

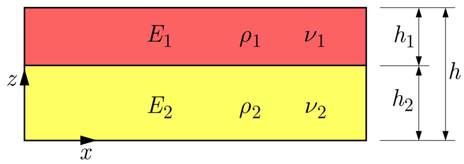

Fig. 1. A scheme of the two-layer plate

Our aim is to construct a gradient plate developed from a two-layer plate as well as to compare the stiffnesses of both systems in the case of any quotient $\eta = h_1/h$.

2.1. Plate geometry

The function describing the properties of the plate is defined as follows

$$p(z) = \left\{ \begin{array}{lll} p_1 & \text{for} & 1 - \eta \leqslant \xi \leqslant 1 \\ p_2 & \text{for} & 0 \leqslant \xi \leqslant 1 - \eta \end{array} \right\} = p_2[1 + \varepsilon s(\xi)] \qquad p = \rho, E, \nu \tag{2.1}$$

where

$$s(\xi) = \begin{cases} 0 & \text{for} \quad 0 \leqslant \xi \leqslant 1 - \eta \\ 1 & \text{for} \quad 1 - \eta \leqslant \xi \leqslant 1 \end{cases} \tag{2.2}$$

where ρ denotes density, E – Young's modulus, ν – Poisson's ratio, $\varepsilon = (p_1 - p_2)/p_2$, $\xi = z/h$, $\eta = h_1/h$, $0 \leqslant \eta \leqslant 1$, $h = h_1 + h_2$. Visualization of the discontinuous function $s(\xi)$ (defined via Eq. (2.2)) is presented in Fig. 2.

We are looking for a continuous-density function $\rho(\xi)$ satisfying the following conditions:
— the law of mass conservation

$$\int\limits_0^1 \rho(\xi)\, d\xi = \frac{\rho_1 h_1 + \rho_2 h_2}{h} = \rho_2(1 + \varepsilon_\rho \eta) \qquad \varepsilon_\rho = \frac{\rho_1 - \rho_2}{\rho_2} \qquad \eta = \frac{h_1}{h} \tag{2.3}$$

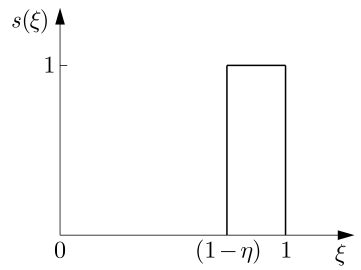

Fig. 2. Discontinuous function $s(\xi)$, see Eq. (1.2)

— positive-density condition

$$\rho(\xi) \geqslant 0 \qquad 0 \leqslant \xi \leqslant 1 \tag{2.4}$$

— boundary conditions

$$\rho(0) = \rho_2 \qquad \rho(1) = \rho_1 \tag{2.5}$$

The function under consideration $\rho(\xi)$ can be described as follows

$$\rho(\xi) = \rho_2[1 + \varepsilon_\rho f(\xi)] \tag{2.6}$$

where the function $f(\xi)$ satisfies the conditions as follows

$$\begin{array}{l} \displaystyle\int\limits_0^1 f(\xi)\;d\xi = \int\limits_0^1 s(\xi)\;d\xi = \eta \\ f(0) = 0 \qquad f(1) = 1 \qquad f(\xi) \geqslant 0 \qquad 0 \leqslant \xi \leqslant 1 \end{array} \tag{2.7}$$

The functions characterizing elastic properties of the FGM material, i.e. Young's modulus $E(\xi)$ and Poisson's ratio $\nu(\xi)$, should satisfy the following conditions

$$\begin{array}{llll} E(\xi) \geqslant 0 & 0 \leqslant \xi \leqslant 1 & E(0) = E_2 & E(1) = E_1 \\ \nu(\xi) \geqslant 0 & 0 \leqslant \xi \leqslant 1 & \nu(0) = \nu_2 & \nu(1) = \nu_1 \end{array} \tag{2.8}$$

The forms of analyzed functions $E(\xi)$ and $\nu(\xi)$ differ. In the case of metallic alloys, one can assume $\nu_1 = \nu_2 = \nu$ because of small differences between Poisson's ratios and the fact that the effect of Poisson's ratio on the deformation is much less than that of Young's modulus (Delale, Erdogan, 1983). However, analyzing the plates, it can be assumed that the function $E(\xi)/[1-\nu^2(\xi)]$ is analogous to the form of the density function expressed by Eq. (2.6)

$$\frac{E(\xi)}{1-\nu^2(\xi)} = \frac{E_2}{1-\nu_2^2}[1 + \varepsilon_E f(\xi)] \qquad \varepsilon_E = \alpha - 1 \qquad \alpha = \frac{E_1(1-\nu_2^2)}{E_2(1-\nu_1^2)} \tag{2.9}$$

and the function $f(\xi)$ satisfies conditions (2.7).

Let us note that taking the function $E(\xi)/[1-\nu^2(\xi)]$ along with conditions $(2.8)_1$ leads to a simple interpretation of the static problem. Tensile strength of the FGM cross-section with Young's modulus and Poisson's ratio described by Eqs. (2.9) is the same as for the cross-section shown in Fig. 1.

Figure 3 shows the functions s and f satisfying conditions (2.7) for $\eta = 0.2$.

We anticipate the following form of $f(\xi)$

$$f(\xi) = f_r(\xi) = \xi^r(a_1\xi + a_2) \tag{2.10}$$

where $r = n$ or $r = 1/n$, and n is an arbitrary natural number.

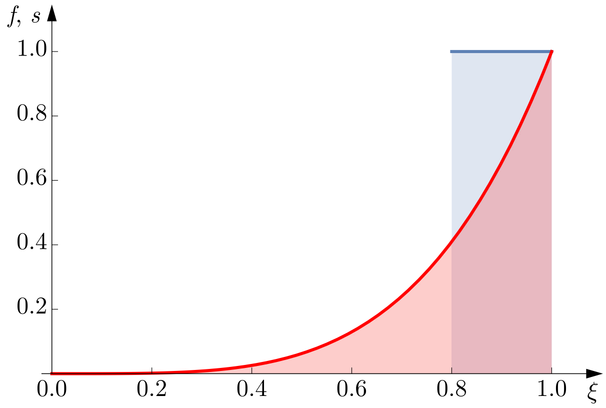

Fig. 3. The functions f and s

The proposed function satisfies boundary condition $(2.7)_2$, whereas condition $(2.7)_3$ is satisfied

$$\forall r \neq 0 \qquad \text{if} \qquad a_2 = 1 - a_1 \quad \Rightarrow \quad f_r(\xi) = \xi^r[a_1(\xi - 1) + 1] \tag{2.11}$$

As a special case $r = n = 0$, condition $(2.7)_3$ will be satisfied with $a_1 = 1$.

Condition $(2.7)_1$ gives

$$\int\limits_0^1 f(\xi)\, d\xi = \int\limits_0^1 \xi^r[a_1(\xi - 1) + 1]\, d\xi = \frac{2 + r - a_1}{(1 + r)(2 + r)} = \eta \tag{2.12}$$

what implies

$$a_1 = (2 + r)[1 - \eta(1 + r)] \tag{2.13}$$

Taking condition $(2.7)_4$

$$\xi^r[a_1(\xi - 1) + 1] \geqslant 0 \tag{2.14}$$

it follows that at $n > 0$, $f(\xi) \geqslant 0$ for

$$-r \leqslant a_1 \leqslant 1 \qquad\qquad \frac{1}{r + 2} \leqslant \eta \leqslant \frac{2}{r + 2} \tag{2.15}$$

It is obvious that for each η, we can find an appropriate natural number n for $r = n$ or $r = 1/n$.

Thus, $f(\xi)$ is written as follows

$$f(\xi) = f_r(\xi) = \xi^r\{1 - (1 - \xi)(2 + r)[1 - \eta(1 + r)]\} \tag{2.16}$$

As a special case of $f_0(\xi)$, we obtain $\eta = 1/2$, $f_0(\xi) = \xi$. Taking $r = 1$

$$f_1(\xi) = \xi[1 - (1 - \xi)3(1 - 2\eta)] \qquad \text{for} \qquad \frac{1}{3} \leqslant \eta \leqslant \frac{2}{3} \tag{2.17}$$

For $n \geqslant 2$, we have two different functions

$$f_n\xi) = \xi^n\{1 - (1 - \xi)(2 + n)[1 - \eta(1 + n)]\} \tag{2.18}$$

or

$$g_n(\xi) = f_{1/n}(\xi) = \xi^{\frac{1}{n}}\Big\{1 - (1 - \xi)\Big(2 + \frac{1}{n}\Big)\Big[1 - \eta\Big(1 + \frac{1}{n}\Big)\Big]\Big\} \tag{2.19}$$

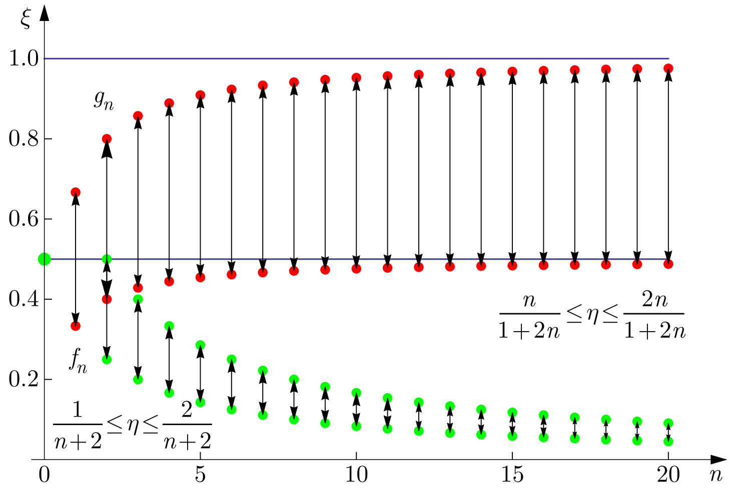

Fig. 4. Ranges of η for $f_n(\xi)$ and $g_n(\xi)$ satisfying conditions (2.7)

For a given value η, one can find such a value n at which the functions $f_n(\xi)$ or $g_n(\xi)$ meet conditions (2.7). Figure 4 shows such ranges of η at which the functions $f_n(\xi)$ and $g_n(\xi)$ satisfy the conditions expressed via Eqs. (2.7).

For $\eta = 1/3$, Fig. 4 depicts four possible values of n, i.e. $n = 1, 2, 3, 4$. On the other hand, we have three functions to be shown in Fig. 5a. In the case of $\eta = 0.2$, we obtain six functions satisfying conditions (2.7) for $n = 3, 4, 5, 6, 7, 8$ (see graphs visualized in Fig. 5b). It is obvious that for any η it gives a collection of functions satisfying conditions (2.7).

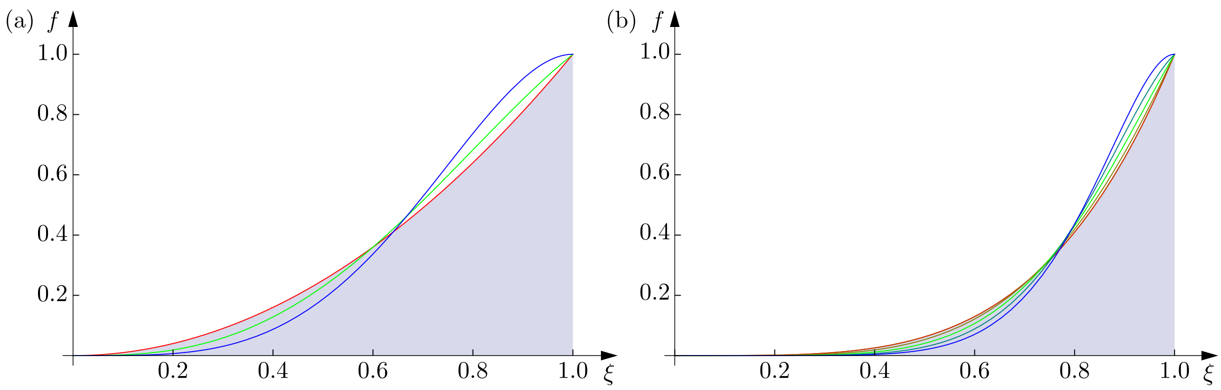

Fig. 5. Graphs of $f_n(\xi)$ for: (a) $\eta = 1/3$ and $n = 1, 2, 3, 4$; (b) $\eta = 0.2$ and $n = 3, 4, 5, 6, 7, 8$

Moving back to the graph illustrated in Fig. 4, it is obvious that for $1/2 \leqslant \eta \leqslant 1$ we get an infinite number of functions satisfying conditions (2.7). Figure 6 shows variation of functions $E(\xi)(1-\nu_2^2)/\{E_2[1-\nu^2(\xi)]\} = 1 + \varepsilon_E f(\xi)$, $f(\xi) = f_n(\xi)$ or $g(\xi) = g_n(\xi)$ for $\alpha = 2$, $\eta = 1/5, 1/6, 1/3$ along the FGM plate thickness.

2.2. Stiffness of the two-layer and FGM plates

The stiffness of the two-layer plate is expressed by the formula

$$D_w = \frac{E_2 h^3}{12(1-\nu^2)} \Big[\eta^3\alpha + (1-\eta)^3 + \frac{3(1-\eta)\alpha\eta}{1-\eta(1-\alpha)}\Big] \tag{2.20}$$

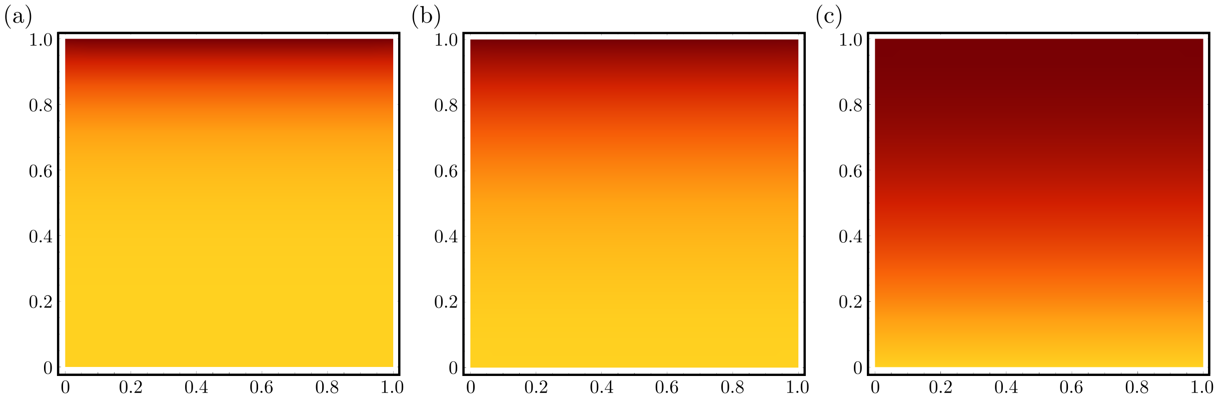

Fig. 6. Cross section of the FGM two-component plate: (a) $\alpha = 2$, $n = 3$, $\eta = 1/5$, (b) $\alpha = 2$, $n = 1$, $\eta = 1/3$, (c) $\alpha = 2$, $n = 1$, $\eta = 2/3$

The stiffness of the FGM plate depends on the functions f or g. These functions depend, in turn, on the variable ξ, on the parameter $\eta = h_1/h$ and on the natural number n

$$E_f(\xi,\alpha,n,\eta) = \frac{E}{1-\nu^2}(\xi,\alpha,n,\eta) = \frac{E_2}{(1-\nu_2^2}[1+(\alpha-1)f_n(\xi)] \tag{2.21}$$

or

$$E_g(\xi,\alpha,n,\eta) = E_f\Big(\xi,\alpha,\frac{1}{n},\eta\Big) = \frac{E_2}{1-\nu_2^2}[1+(\alpha-1)g_n(\xi)] \tag{2.22}$$

The stiffness of the FGM plate material is expressed via formulas:
— for $\frac{1}{n+2} \leqslant \eta \leqslant \frac{2}{n+2}$

$$\begin{aligned} D_{f(FGM)}(\alpha,n,\eta) &= \frac{E_2h^3}{1-\nu_2^2} \int\limits_{-e_f}^{1-e_f} [1+(\alpha-1)f_n(\xi+e_f)]\xi^2\,d\xi \\ &= \frac{1}{3} - e_f + e_f^2 + (\alpha-1)\Big(\eta e_f^2 + \frac{2+(1+n)(2+n)\eta}{(3+n)(4+n)} - \frac{2e_f[1+(1+n)(2+n)\eta]}{(2+n)(3+n)}\Big) \end{aligned} \tag{2.23}$$

— for $\frac{n}{1+2n} \leqslant \eta \leqslant \frac{2n}{1+2n}$

$$\begin{aligned} D_{g(FGM)}(\alpha,n,\eta) &= D_{f(FGM)}\Big(\alpha,\frac{1}{n},\eta\Big) = \frac{E_2h^3}{1-\nu_2^2} \int\limits_{-e_g}^{1-e_g} [1+(\alpha-1)g(\xi+e_g)]\xi^2\,d\xi = \frac{1}{3} - e_g \\ &+ e_g^2 + (\alpha-1)\Big(\frac{2n^2+\eta\{(1-e_g)[1-e_g+n(3-7e_g)]+2n^2(1-4e_g+6e_g^2)\}}{(1+3n)(1+4n)} \\ &- \frac{2n^2e_g}{(1+2n)(1+3n)}\Big) \end{aligned} \tag{2.24}$$

whereas

$$\begin{aligned} e_f(\alpha,\eta,n) &= \frac{4+5n+n^2+2\alpha+2(1+n)(2+n)(\alpha-1)\eta}{2(2+n)(3+n)[1+(\alpha-1)\eta]} \\ e_g = e_f\Big(\alpha,\eta,\frac{1}{n}\Big) &= \frac{1+5n+4n^2+2n^2\alpha+2(1+n)(1+2n)(\alpha-1)\eta}{2(2n+1)(3n+1)[1+(\alpha-1)\eta]} \end{aligned} \tag{2.25}$$

In general, we have the following inequalities

$$
\begin{aligned}
&D_{f(FGM)}\Big(\alpha,n,\eta=\frac{2}{2+n}\Big)\neq D_{f(FGM)}\Big(\alpha,n+1,\eta=\frac{1}{2+n}\Big)\\
&D_{g(FGM)}\Big(\alpha,n,\eta=\frac{2n}{2n+1}\Big)\neq D_{g(FGM)}\Big(\alpha,n+1,\eta=\frac{n}{2n+1}\Big)
\end{aligned}
\tag{2.26}
$$

but there always exists such $\widehat{\eta}$ meeting the following equality for each α

$$
D_{FGM}(\alpha,n,\widehat{\eta})=D_{FGM}(\alpha,n+1,\widehat{\eta})
\tag{2.27}
$$

For each α, the following equality is satisfied

$$
D_{f(FGM)}\Big(\alpha,n,\eta=\frac{1}{2+n}\Big)=D_{f(FGM)}\Big(\alpha,n+1,\eta=\frac{1}{2+n}\Big)
\tag{2.28}
$$

In the case of $n/(1+2n)\leqslant\eta\leqslant 2n/(1+2n)$, there exist such values of $\widehat{\eta}$ satisfying the following equalities

$$
D_{g(FGM)}(\alpha,n,\widehat{\eta})=D_{g(FGM)}(\alpha,n+1,\widehat{\eta})
\tag{2.29}
$$

For example: $D_{g(FGM)}(\alpha=2,n=1,\widehat{\eta})=D_{g(FGM)}(\alpha=2,n=2,\widehat{\eta})$, for $\widehat{\eta}=0.424472$.

Figure 7 presents diagrams of the function $r(\eta)$ describing the stiffness of the plate $D=E_2h^3r(\eta)/[12(1-\nu_2^2)]$ for $\alpha=2$ where D_w and D_{FGM} denote the two-layer plate and the graded material plate, respectively.

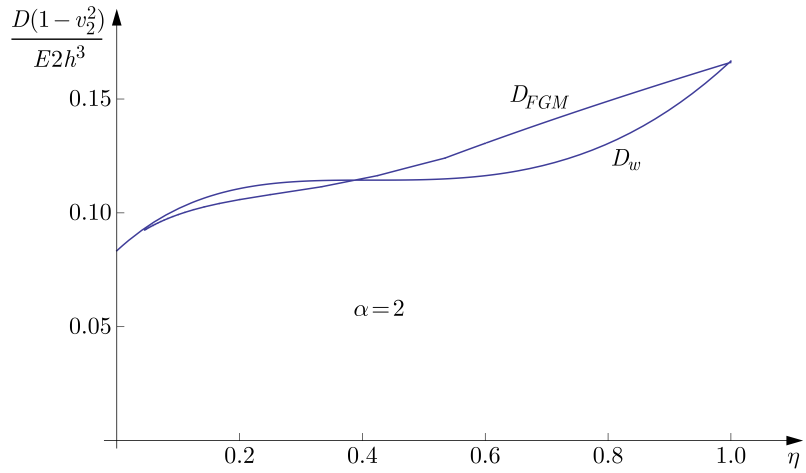

Fig. 7. A diagram of the function $r(\eta)$

3. Modelling of the gradient plate developed from the three-layer plate

Let us consider a three-layer plate with a symmetrical arrangement of layers. In such a case, it is convenient to take the intermediate layer thickness equal to $2h_2$ (Fig. 8).

3.1. Determining the functions f_n, g_n

Similarly, as in the case of two-layer plate, we assume that Eqs. (2.9) hold provided that the functions f_n and g_n have the following forms

$$
f_n(\xi)=\xi^{2n}[1-a_1(1-\xi^2)] \qquad g_n(\xi)=(\xi^2)^{\frac{1}{n}}[1-b_1(1-\xi^2)]
\tag{3.1}
$$

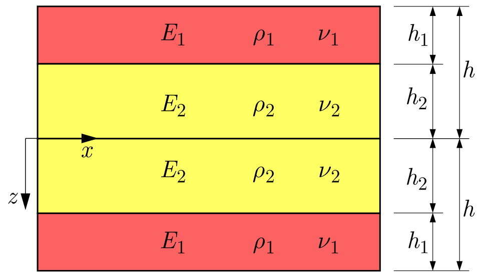

Fig. 8. A scheme of the three-layer plate

Satisfying the following conditions (see (2.7))

$$\begin{aligned}
&\int\limits_0^1 f(\xi)\,d\xi = \int\limits_0^1 s(\xi)\,d\xi = \eta = \frac{h_1}{h} \\
&f(\pm 1) = 1 \qquad f(0) = 0 \qquad f(\xi) \geqslant 0 \qquad -1 \leqslant \xi \leqslant 1
\end{aligned} \tag{3.2}$$

we obtain the functions f_n and g_n of the form:

— for $\frac{1}{3+2n} \leqslant \eta \leqslant \frac{3+4n}{(1+2n)(3+2n)}$

$$f_n(\xi) = \xi^2 n\Big(1 - \frac{1}{2}(3+2n)[1 - \eta(1+2n)](1-\xi^2)\Big) \tag{3.3}$$

— for $\frac{n}{2+3n} \leqslant \eta \leqslant \frac{n(3n+4)}{(2+n)(2+3n)}$

$$g_n(\xi) = f_{1/n}(\xi) = (\xi^2)^{\frac{1}{n}}\Big(1 - \frac{1}{2n^2}(2+3n)[n(1-\eta) - 2\eta](1-\xi^2)\Big) \tag{3.4}$$

Figure 9 shows the ranges of η for the functions $f_n(\xi)$ and $g_n(\xi)$ satisfying conditions (2.7).

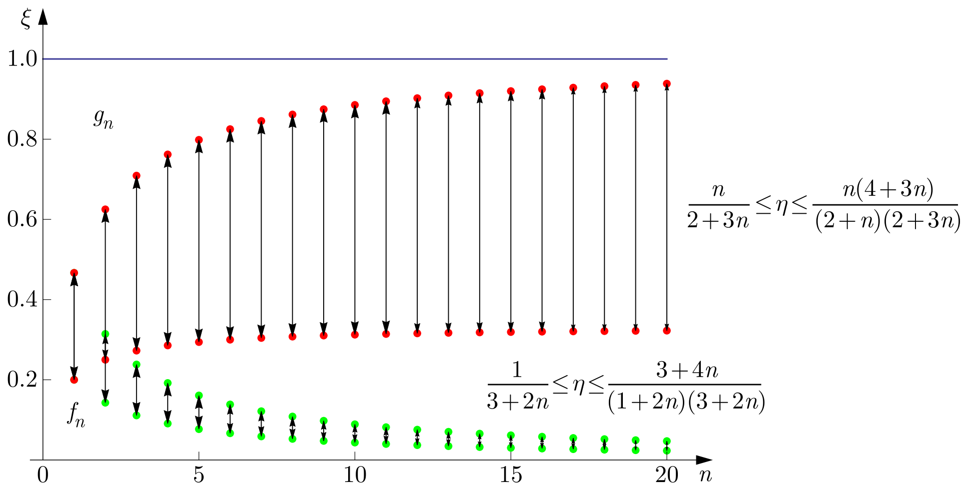

Fig. 9. Ranges of η for $f_n(\xi)$ and $g_n(\xi)$ satisfying conditions (2.7)

Figure 10a presents functions $f_1 = g_1$ within the range of validity $3/15 \leqslant \eta \leqslant 7/15$, whereas the functions g_{10} for $30/96 \leqslant \eta \leqslant 85/96$ are visualized in Fig. 10b.

Similarly, as in Section 3, the function $E(\xi)/[1 - \nu^2(\xi)]$ can be expressed as follows

$$\frac{E(\xi)}{1 - \nu^2(\xi)} = \frac{E_2}{1 - \nu_2^2}[1 + \varepsilon_E f(\xi)] \tag{3.5}$$

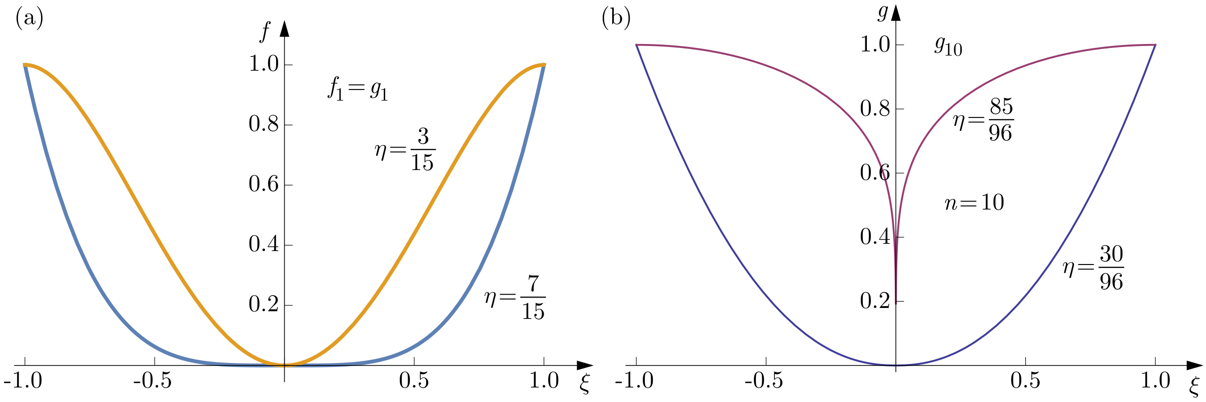

Fig. 10. (a) Functions $f_1 = g_1$ for $3/15 \leqslant \eta \leqslant 7/15$, (b) functions g_{10} for $30/96 \leqslant \eta \leqslant 85/96$

where the following designations are adopted

$$\varepsilon_E = \alpha - 1 \qquad \alpha = \frac{E_1(1-\nu_2^2)}{E_2(1-\nu_1^2)} \qquad f(\xi) = f_n(\xi) \quad \text{or} \quad f(\xi) = g_n(\xi) \tag{3.6}$$

Figure 11 presents variations of the function $E(\xi)(1-\nu_2^2)/\{E_2[1-\nu^2(\xi)]\} = 1 + \varepsilon_E f(\xi)$, $f(\xi) = f_n(\xi)$ or $g(\xi) = g_n(\xi)$ for $\alpha = 2$, $\eta = 1/5, 7/15, 5/8$ along the FGM plate thickness.

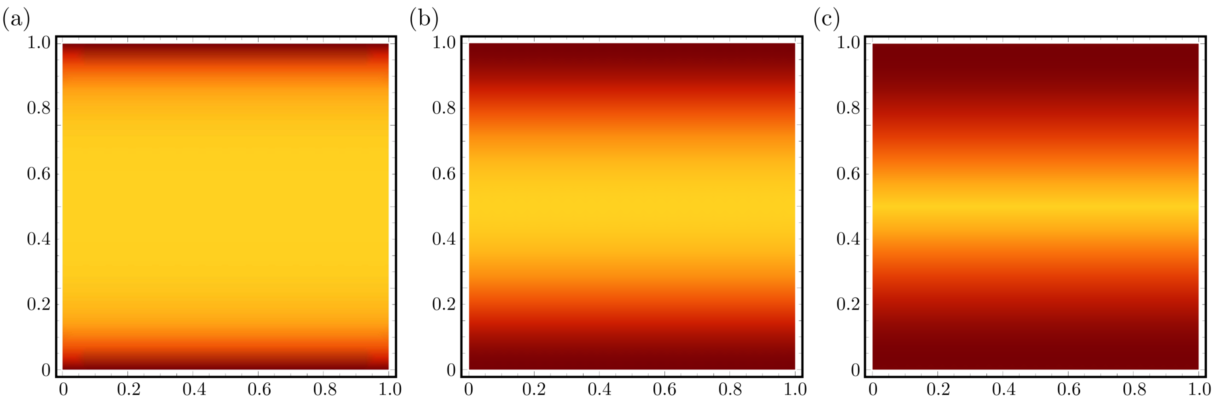

Fig. 11. Cross section of the FGM two-component plate: (a) $f_1(\alpha = 2, \eta = 1/5)$, (b) $f_1(\alpha = 2, \eta = 7/15)$, (c) $g_2(\alpha = 2, \eta = 5/8)$

3.2. Stiffness of the three-layer FGM plate

The stiffness of the three-layer plate D_w can be described as follows

$$D_w = \frac{2E_2h^3}{3(1-\nu_2^2)}[(1-\eta)^3 + \alpha\eta(3 - 3\eta + \eta^2)] \tag{3.7}$$

In the case of the FGM plate, the following formulas can be applied:
— for $\frac{1}{3+2n} \leqslant \eta \leqslant \frac{3+4n}{(1+2n)(3+2n)}$

$$D_{f(FGM)}(\alpha, n, \eta) = \frac{2E_2h^3}{3(1-\nu_2^2)} \frac{3(3+2\alpha) + 4n(4+n) + 3\eta(\alpha-1)[3+4n(2+n)]}{(3+2n)(5+2n)} \tag{3.8}$$

— for $\frac{n}{2+3n} \leqslant \eta \leqslant \frac{n(4+3n)}{(2+n)(2+3n)}$

$$D_{g(FGM)}(\alpha, n, \eta) = \frac{2E_2h^3}{3(1-\nu_2^2)} \frac{4 + 16n + 9n^2 + 6\alpha n^2 - 3\eta(2+n)(2+3n)(\alpha-1)}{(2+3n)(2+5n)} \tag{3.9}$$

The stiffnesses of the layered plate D_w and the FGM plate D_{FGM} as a function of η for $\alpha = E_1/E_2 = 2$ are visualized in Fig. 12.

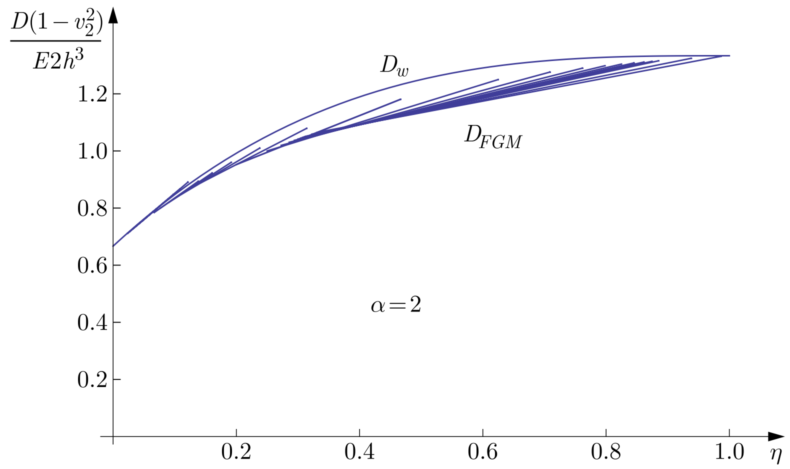

Fig. 12. Layered plate stiffness D_w and FGM plate stiffness D_{FGM} as a function of η for $\alpha = E_1/E_2 = 2$

4. Conclusions

Figure 7 shows the dependence of the stiffness of a two-layer plate and an FGM plate on the parameter η. Analyzing this graph, one concludes that taking two plates (the two-layer and FGM) with the same amount of the material and for certain values of the parameter η, the stiffness of the FGM plate is greater than the stiffness of the two-layer plate. It proves that we can construct an FGM plate, according to the procedure outlined in Section 2, with a higher stiffness of the two-layer plate and with the same amount of the material for both plates. In the case of the three-layer plate and its corresponding FGM plate, the FGM plate stiffness is less than the stiffness of the three-layer plate for all values of the parameter η, except for $\eta = 0$ and $\eta = 1$, for which the stiffnesses are the same.

References

1. Delale F., Erdogan F., 1983, The crack problem for a nonhomogeneous plane, *ASME Journal of Applied Mechanics*, **50**, 609-615
2. Efraim E., 2011, Accurate formula for determination of natural frequencies of FGM plates basing on frequencies of isotropic plates, *Procedia Engineering*, **10**, 242-247
3. Kim J., Reddy J.N., 2014, Analytical solutions for bending, vibration, and buckling of FGM plates using a couple stress-based third-order theory, *Composite Structures*, **103**, 86-98
4. Kumar J.S., Reddy B.S., Reddy C.E., Kumar Reddy K.V., 2011, Geometrically non linear analysis of functionally graded material plates using higher order theory, *International Journal of Engineering Science and Technology*, **3**, 1, 279-288
5. Mahamood R.M., Esther T. Akinlabi E.T., Shukla M., Pityana S., 2012, Functionally graded material: an overview, *Proceedings of the World Congress on Engineering, WCE 2012*, **III**, London, U.K.
6. Mokhtar B., Abedlouahed T, Abbas A.B., Abdelkader M., 2009, Buckling analysis of functionally graded plates with simply supported edges, *Leonardo Journal of Sciences*, **16**, 21-32

7. Nagórko W., 1998, Two methods of modeling of periodic nonhomogeneous elastic plates, *Journal of Theoretical and Applied Mechanics*, **36**, 291-303

8. Nagórko W., 2010, Asymptotic modeling in elastodynamics of FGM, [In:] *Mathematical Modelling and Analysis in Continuum Mechanics of Microstructured Media*, Woźniak C. et al. (Edit.), Silesian University of Technology, Gliwice, 143-151

9. Reddy J.N., 2000, Analysis of functionally graded plates, *International Journal for Numerical Methods in Engineering*, **47**, 663-684

10. Rohit Saha, Maiti P.R., 2012, Buckling of simply supported FGM plates under uniax ial load, *Iternational Journal of Civil and Structural Engineering*, **2**, 4, 1035-1050

11. Wągrowska M., Woźniak C., 2015, A new 2D-model of the heat conduction in multilayered medium-thickness plates, *Scientiarum Polonorum Acta Architectura*, **14**, 1, 37-44

12. Woźniak C., 1995, Microdynamics: continuum modeling the simple composite materials, *Journal of Theoretical and Applied Mechanics*, **33**, 267-289

13. Woźniak C., Wągrowska M., Szlachetka O., 2016, On the tolerance modelling of heat conduction in functionally graded laminated media, *Journal of Applied Mechanics and Technical Physics*, **56**, 2, 274-281

Manuscript received August 22, 2016; accepted for print February 7, 2018